Chapter 6

Investigation into the innate immune responses to rotavirus transcripts

6.0 Introduction

The innate immune response to viruses, especially RNA viruses, is the first line of defence in controlling these viral pathogens (Randall and Goodbourn, 2008). The innate immune response is mainly characterised by the secretion of interferon (IFN) which is induced by pathogen associated molecular patterns (PAMPs) via several pathogen pattern recognition receptors (PRRs) (Takeuchi and Akira, 2009). The PRRs include the cytoplasmic retinoic-acid inducible gene I-like receptors (RLRs), membrane-bound Toll-like receptors (TLRs) and the cytoplasmic nucleotide oligomerisation domain (NOD)-like receptors (Akira *et al.*, 2006, Mogensen, 2009). The RLRs include the retinoic acid-inducible gene I (RIG-I), the melanoma differentiation associated gene 5 (MDA5) and the laboratory of physiology and genetics gene 2 (LPG2) (Saito *et al*., 2007, Pippig *et al*., 2009, Loo *et al*., 2008). RIG-I and MDA5 contain two caspase activation and recruitment domains (CARDs) at the N-terminal ends (Figure 6.1) (Luo *et al.*, 2011). At the C-terminus of RIG-I and MDA5 is a DExD/H-box helicase domain (Figure 6.1) that unwinds dsRNA through its ATPase activity (Hirata *et al*., 2007, Broquet *et al*., 2011, Yoneyama *et al*., 2005, Pippig *et al*., 2009, Luo *et al*., 2011). The LPG2 lacks CARD domains, but also contains a similar helicase domain (Figure 6.1B) which recognises the termini of dsRNA (Li *et al*., 2009a). Although the specific function of LPG2 is not clear, it is thought to be a negative regulator of RIG-I and MDA5 (Komuro *et al*., 2008). Three helicase domains (HEL1, HEL2 and insertion HEL2i) which contain motifs I–VI (Figure 6.1B) are conserved between RIG-I, MDA5 and LPG2, and clasp dsRNA through a network dominated by polar contacts (Luo *et al*., 2011). RIG-I is activated upon binding to viral dsRNA or RNA with 5'-triphosphates. Stimulated RIG-I subsequently recruits the adapter protein IFN promoter-stimulator 1 (IPS) which is also known as the mitochondrial antiviral signalling (MAVS) adapter protein (Lei *et al*., 2009). The recruitment of IPS/MAVS lead to the induction of several transcription

factors including interferon regulatory factors 3 and 7 (IRF-3, IRF-7) and NF-κB resulting in the production of type I IFN and inflammatory factors (Fujita *et al*., 2007).

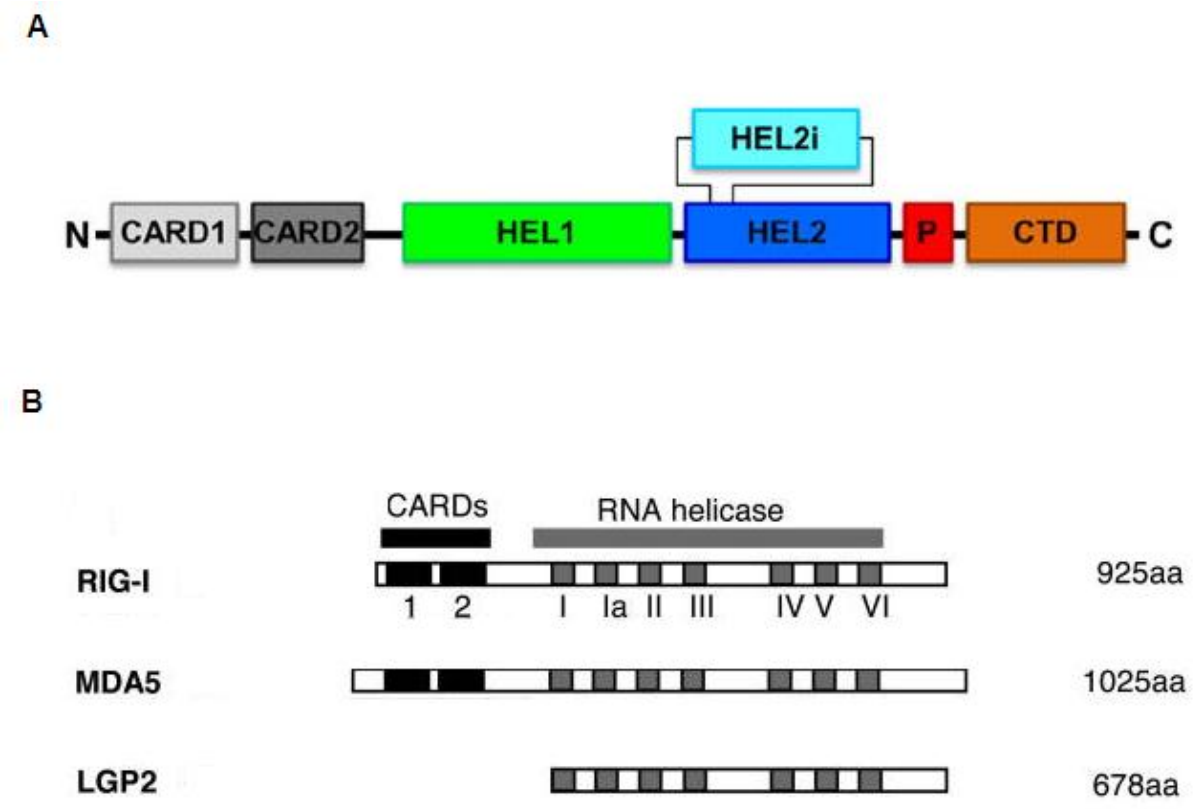

Figure 6.1. Schematic illustration of the domain structures of the retinoic-acid inducible gene I-like receptors (RLRs). A, A representation of RIG-I showing the caspase activation and recruitment domains (CARD 1 and 2) and three helicase domains (HEL1, HEL2 and HEL2i) that clasp dsRNA. HEL2i is an α-helical insertion structure which is important for specific recognition and gripping dsRNA by binding to the minor groove of the RNA backbone. The pincer region (red) connects the functional domains of HEL1, HEL2 and the C-terminal domain (CTD) to facilitate communication between them. **B**, A graphical illustration depicting the differences between RIG-I, MDA5 and LPG-2. LPG2 lacks the CARD domains. Conserved between the RLRs are RNA helicase motifs I–VI, which are shown in gray. The number of amino acids in each RLR is indicated at the right. Figure adapted from Saito *et al*., 2007 and Luo *et al*., 2011 with permission from the publishers.

The IFN response is an early response which occurs before the adaptive immune response (Samuel, 2001). In viral infections, innate immune responses induce an antiviral state which enables the destruction of virus-infected cells through cell death pathways such as apoptosis, programmed necrosis (necroptosis) as well as the modulation of the immune system by activation of effector cells (Stetson and

Medzhitov, 2006, Seth *et al*., 2006, Levy *et al*., 2011, Samuel, 2001, Edinger and Thompson, 2004, Galluzzi and Kroemer, 2008). The antiviral state is achieved via several mechanisms and include the inhibition of mRNA translation (through PKR), RNA degradation though the activation of oligoadenylate synthetase which prevents translation (Stark *et al*., 1998) and RNA editing by adenosine deaminase (Figure 6.2).

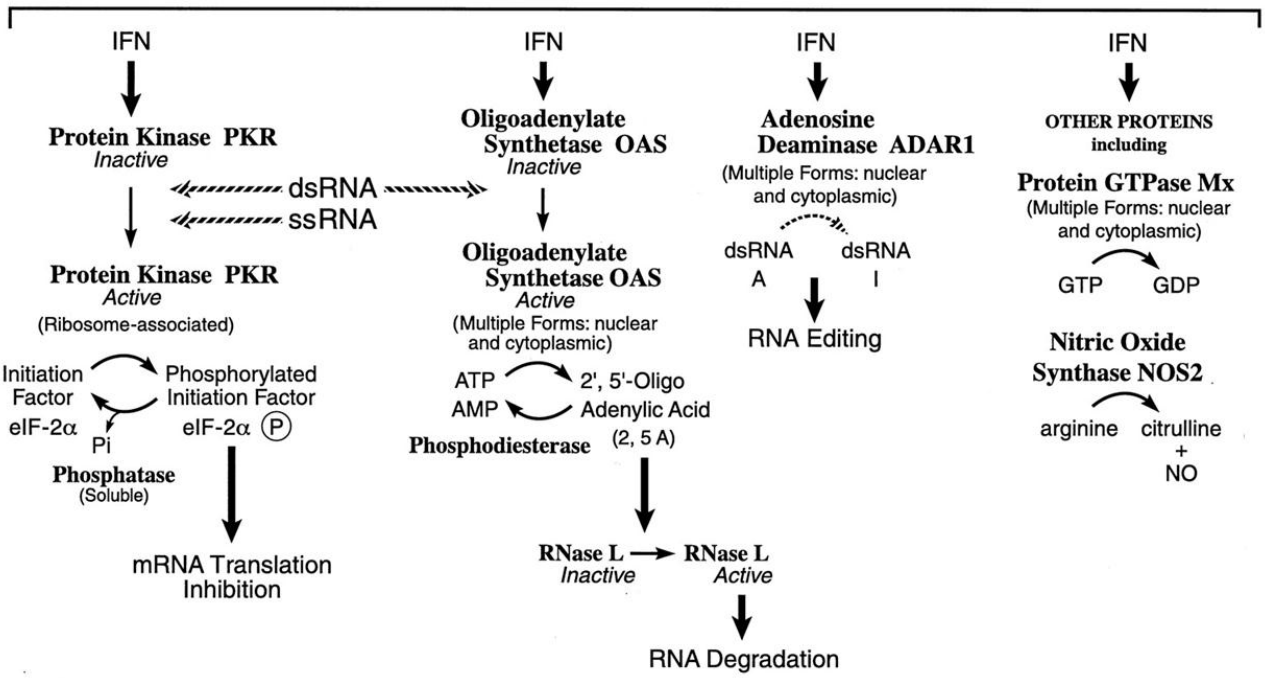

Figure 6.2. Interferon pathways that induce an antiviral state in response to viral pathogen associated molecular patterns. Figure adapted from Samuel, 2001 with permission from the publisher.

The innate immune response to rotavirus infection depends on the strain and host-cell type (Frias *et al*., 2010, Sen *et al*., 2011, Frias *et al*., 2012). For instance, in intestinal epithelial cells, rotavirus-stimulated IFN type I (IFN-α; IFN-β) induces anti-viral signalling and apoptosis (Frias *et al*., 2012). However, rotavirus NSP1 antagonises IFN-mediated antiviral responses by degrading IRF-3, IRF-5, IRF-7, β-TrCP (which inhibits NF-κB) as well as inhibiting RIG-I (Sen *et al*., 2009, Graff *et al*., 2009, Graff *et al*., 2002, Qin *et al*., 2011, Barro and Patton, 2005, Barro and Patton, 2007). A study investigating the innate immune response in neonatal gnotobiotic piglets showed that high levels of IFN-α and interleukin (IL) 12 were induced

(Gonzalez *et al*., 2010). The induction of IFN-α in plasmacytoid dendritic cells (pDCs) was shown to require dsRNA, VP4 and or VP7 (Deal *et al*., 2010). Both live and inactivated rhesus rotavirus efficiently stimulate the secretion of type I IFN in pDCs (Deal *et al*., 2010). While the observation that inactivated rotavirus stimulates IFN induction suggests that transcription is not required for rotavirus recognition in pDCs, replication is required for type I IFN production in fibroblasts (Clark *et al*., 2010, Feng *et al*., 2009). In mice, genomic rotavirus dsRNA was shown to induce severe intestinal injury in a TLR3-recognition pathway (Zhou *et al*., 2007a). Using the simian rotavirus RRV (including its dsRNA) and bovine rotavirus UK strains, the early innate immune response and secretion of IFN in mouse embryonic fibroblasts (MEFs) and RIG-I, MDA5 or double-knockout mice, was found to be dependent on IPS/MAVS (Sen *et al*., 2011). However, neither RIG-I nor MDA5 was found to be essential for rotavirus mediated IFN production, but both contributed to IFN production. A proposed model of events thought to occur during early innate immune recognition of rotaviruses is shown in Figure 6.3 (Sen *et al*., 2011). The dsRNA-dependent kinase (PKR) is directly activated by dsRNA but is also IFN-inducible (Kaempfer, 2006, Lemaire *et al*., 2008). Although PKR was found to be essential for the production of IFN-β in rotavirus-infected cells, it was apparently not required for the early antiviral transcriptional response to rotavirus and the secretion of IFN-α or lFN-β (Figure 6.3) (Sen *et al*., 2011). STAT1, STAT3 and IRF9 are also known to be activated in the pathway (Section 2.4; Figure 2.7).

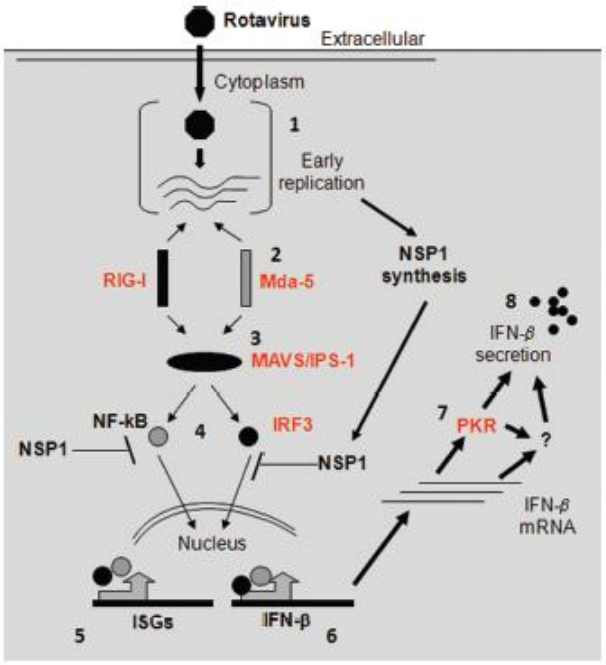

Figure 6.3. A proposed model of events occurring during early innate immune recognition of rotavirus leading to IFN production. The numbers refer to the different steps in the pathway. Parts of the pathway indicated in red were determined by Sen et al., 2011 while the rest of the pathway is based on the findings of others (Barro and Patton, 2007, Feng *et al*., 2009, Hirata *et al*., 2007). In this model, rotavirus genetic material is sensed by both MDA5 and RIG-I. The interferon antagonist NSP1 acts by inhibiting NF-κB and interferon regulatory factor 3 (IRF3). Figure from Sen *et al*., 2011 with permission from the publisher.

In this study, rotavirus DS-1 transcripts which were obtained from *in vitro* transcription of the consensus genome cDNA by T7 polymerase, and rotavirus SA11 mRNA obtained from *in vitro* transcription using double-layered particles (DLPs) were transfected into BSR and COS-7 cells in an attempt to recover viable rotavirus by the transcript-based reverse genetics approach (chapter 5). The effect of inhibiting PKR was also investigated based on indications that the modulation of the innate immune system with the PKR inhibitor, 2-aminopurine (2-AP), improved the efficiency of recovering bluetongue virus in BSR cells (Attoui *et al*., 2009). However, the use of a consensus sequence, inhibition of PKR with 2-AP or imidazolo-oxindole PKR inhibitor C16 in this study did not result in the recovery of viable rotavirus. The transfection of double-layered particle (DLP)-derived rotavirus SA11 mRNA also failed. The transfection of *in vitro* derived rotavirus DS-1 and SA11 transcripts induced a consistent pattern of cell death (chapter 5; Tables 5.3 and 5.4). Taken together, it was hypothesised that the presence of rotavirus genetic material in cells,

in the absence of virus particles, induced an antiviral state due to innate immune responses. This may severely impair the adequate synthesis of rotavirus proteins, coordinated replication and packaging of the rotavirus genome to produce rotavirus particles. The induction of the anti-rotavirus mechanism could probably follow any of the mechanisms shown in Figure 6.2. Several studies have used triple-layered particles (TLPs), DLPs and dsRNA to understand host innate immune responses in cell culture (Sen *et al.*, 2011, Frias *et al*., 2012, Deal *et al*., 2010) However, the specific innate immune responses to single-stranded rotavirus transcripts have not been reported to date. The results described in chapter 5 indicated that the transcripts were responsible for innate immune-induced apoptotic cell death. Apoptotic cell death has also been reported for African horse-sickness virus-infected cells (Stassen *et al.*, 2012). Therefore, the objective of this chapter was to identify and characterise the innate immune response to rotavirus transcripts.

A human cell line, HEK 293H cells (a variant of HEK 293 cells), was selected for investigation of innate immune responses due to the availability of human gene expression assays and also that the cells can be transfected efficiently (Preuss *et al*., 2000). The experimental approach was to transfect HEK 293H with *in vitro* derived rotavirus DS-1 and SA11 transcripts followed by determining the expression levels of selected cytokines using qRT-PCR with TaqMan® Gene Expression Assays and western blot analyses. IFN-α, IFN-1β and IFN-λ1 were selected since they are the major cytokines of type I (IFN-α, IFN-1β) and type III (IFN-λ1) IFN systems. The probes against the interferon genes, IL12 p40 and TNF-α were selected due to their potent antiviral activities (Ramshaw *et al*., 1997). In addition, TNF-α is a pro-inflammatory cytokine which is cytotoxic and contributes to cell injury (Horiuchi *et al*., 2010). Therefore, a probe for the detection of the anti-inflammatory *IL10* mRNA was used to determine if the cells attempted to suppress any TNF-α activity. CXCL10 is an interferon-induced cytokine which is also associated with anti-cell proliferation activity (Campanella *et al*., 2010).

6.1 Materials and methods

6.1.1 Cells and transcripts

HEK 293H cells were maintained in Dulbecco's modified Eagle's medium (Hyclone) containing 1% penicillin/streptomycin/amphotericin (Lonza), and supplemented with 1% non-essential amino acids (Gibco) and 10% foetal bovine serum (Hyclone). The HEK 293H cells were kindly provided by Dr. A. C. Potgieter (Deltamune). Rotavirus DS-1 and SA11 transcripts were obtained from *in vitro* transcription as described in chapter 5 (section 5.1.6).

6.1.2 Quantitative RT-PCR

HEK 293H cells were grown to 80% confluence in wells of 6-well plates (Nunc^{TM}) followed by transfection using Lipofectamine$^{®}$ 2000 (Invitrogen), in duplicate, with 1.5 µg of synthetic rotavirus DS-1 genome segment 6 mRNA (DS-1 GS6), wild-type rotavirus SA11 mRNA (SA11 mRNA) or synthetic BTV-1 S3 mRNA (BTV-1 S3). A single transfection was performed and the cells were incubated for 10 hours at 37 ^{o}C and 5% CO_2. For each transcript transfected, the HEK 293H cells from the duplicate wells were pooled and total cellular RNA was extracted using TRI-Reagent LS (Molecular Research Centre). cDNA was synthesised using the High Capacity RNA-to-cDNA master mix (Applied Biosystems). The cDNA synthesis reaction was incubated at 25 ^{o}C for 5 minutes followed by 30 minutes at 42 ^{o}C. The reverse transcriptase was inactivated by heating at 85 ^{o}C for 5 minutes. PCR amplification of cDNA was performed using a TaqMan Universal PCR Master Mix buffer and commercial probes. The selected probes were for *IFN-λ1* (assay ID: Hs00601677_gl), *IFN-1β* (Hs00277188_sl), *IFN-α1* (Hs00256882_s1), *TNF-α* (Hs00174128_ml), anti-inflammatory *IL10* (Hs00961622m1), Th1-type *IL12 p40* (Hs00233688_ml), IFN-inducible *CXCL10* (Hs00171042_ml), and the receptor-interacting protein 1 (*RIP1*) kinase (Hs00169407_m1). All the TaqMan assays were purchased from Applied Biosystems. Three independent experiments were performed and real-time PCR amplification for each independent experiment was conducted in triplicate with an AB7500 thermo cycler. Relative quantities of cytokine RNA were normalised to *β-actin* (Applied Biosystems) mRNA using the $2^{-\Delta\Delta C}{}_{T}$ method (Livak and Schmittgen, 2001).

6.1.3 Western blot analyses

HEK 293H cells were transfected as described in Section 6.1.2 followed by the preparation of whole-cell lysates with NP-40 buffer (1% NP-40, 50 mM Tris/HCl pH 8.0 and 150 mM NaCl). The lysis buffer also contained 1X Complete Protease Inhibitor cocktail (Roche). Proteins in the lysate were separated using 10% SDS-PAGE followed by protein transfer onto nitrocellulose membranes (Whatman^{TM}). Transfer was achieved at 100 volts for 1 hour in a transfer buffer containing 0.025 M Tris, 0.2 M glycine and 20% methanol (pH 8.4). To verify that proteins had successfully transferred, the membrane was briefly stained with Ponceau S solution (Fluka). The membranes were blocked with 5% skimmed milk (Nestle) in 1 X Tris buffered saline with Tween-20 (TBST) for 1 hour at 4 ^{o}C with constant agitation. The milk was briefly rinsed with 1X TBST and five separate nitrocellulose membranes were incubated with anti-IRF3, anti-IRF7, anti-PARP-I, anti-MDA5 or rabbit anti-RIG-I primary antibodies (Santa Cruz) for 16 hours at 4 ^{o}C with shaking at 140 rpm. The anti-GAPDH antibody (AbD Serotec) was used on a separate immunoblot as a control and all the primary antibodies were used at a 1:1000 dilution. For MDA5, a 36.2 kDa peptide corresponding to amino acids 928–1023 of the human MDA5 (Abcam) was used as a positive control. Unbound primary antibodies were washed away five times with 1X TBST followed by incubation with either anti-mouse or anti-rabbit secondary antibodies (Santa-Cruz) for 4 hours at 4 ^{o}C. The secondary antibodies were used at a dilution of 1:1000. To develop bands on the membrane, a 4-chloro-1-Naphtol peroxidase substrate tablet (Sigma) was dissolved in 10 ml ice-cold methanol. A 2 ml volume of the dissolved substrate was added to 10 ml PBS (pH 7.4) followed by the addition of 5 µl of H_2O_2 (Sigma). The complete membrane-development solution was applied onto the nitrocellulose for 5 minutes or until bands were sufficiently developed. Further development was stopped by transferring the membrane into deionised water.

6.1.4 Determination of the extent of PKR inhibition

To determine the level of PKR inhibition with imidazolo-oxindole, 2 µg of purified rotavirus SA11 dsRNA was transfected into HEK 293H cells in a well (10 cm^2) of a six-well plate (Nunc^{TM}). The dsRNA transfection was performed into cells in which PKR was either not inhibited or was inhibited with 20 µM imidazolo-oxindole (Sigma).

A mock transfection was also performed. The transfected cells were incubated at 37 ^{o}C and 5% CO_2 for 10 hours followed by cell lysis and a western blot using the anti-pPKR antibody (Santa-Cruz) at a 1:1000 dilution. The cell lysis and western blot procedures were as described in section 6.1.3 above.

6.2 Results

6.2.1 Identification of the rotavirus transcript-sensor in HEK 293H cells

Due to the identified roles of RIG-I and MDA5 in sensing viral RNA (Yoneyama *et al*., 2005, Fujita *et al*., 2007), and the results obtained in chapter 5 which suggested the role of RIG-I in response to transfection of rotavirus mRNA, it was decided to investigate if rotavirus transcripts were sensed by RIG-I, MDA5 or both. Analysis of the expression of RIG-I and MDA5 in HEK 293H cells, in response to the transfection of rotavirus or bluetongue virus transcripts was performed by western blot analysis. RIG-I was detected in cells which were transfected with synthetic rotavirus DS-1, wild type rotavirus SA11 and BTV-1 transcripts, but not in the mock-transfected cells (Figure 6.4A). MDA5 expression was not detectable in the mock-transfected cells as well as cells that were transfected with synthetic rotavirus DS-1, wild type rotavirus SA11 or BTV-1 transcripts (Figure 6.4A). A human MDA5 peptide used as a positive control was detected using the anti-MDA5 antibody (Figure 6.4B). This result confirmed that the lack of detection of MDA5 in the mock- and transcript-transfected cells was a true negative result and not due to antibody failure.

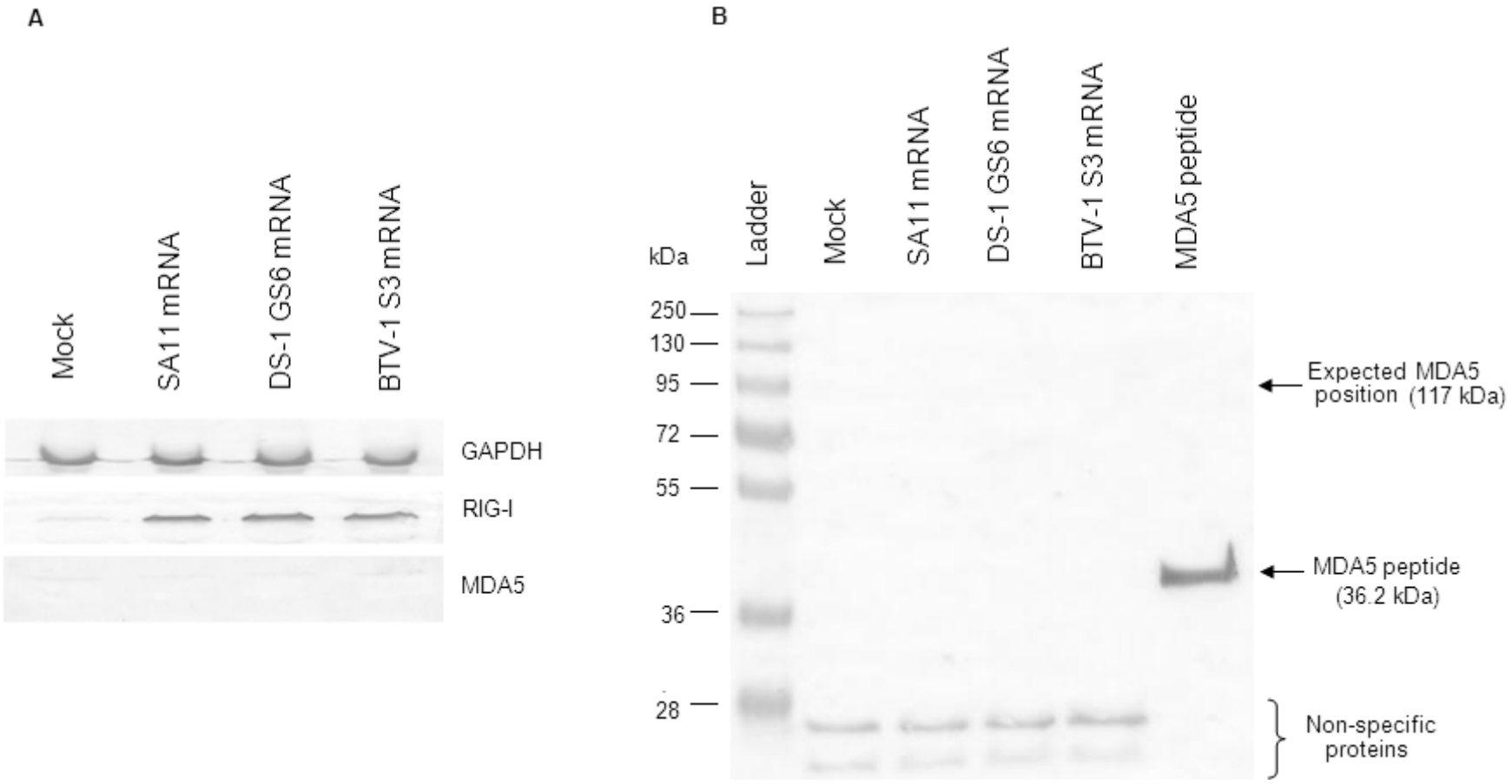

Figure 6.4. Western blot analysis of retinoic acid-inducible gene I (RIG-I) and melanoma differentiation-associated gene 5 (MDA5) expression following the transfection of HEK 293H cells with rotavirus DS-1 genome segment 6 (VP6), rotavirus SA11 and BTV-1 segment 3 (VP3) transcripts. The transcripts transfected into HEK 293H cells are indicated at the top of each lane. **A**, Western blot analysis indicating that RIG-I (middle strip) but not MDA5 (bottom strip) is expressed in response to viral transcripts. A GAPDH control was included for each transfection (top strip). **B**, Western blot analysis of the expression of MDA5. The immunoblot was performed with a human MDA5-peptide positive control. The protein size marker is a PageRuler^{TM} Plus prestained protein ladder (Fermentas).

6.2.2 The interferon response of HEK 293H cells to rotavirus transcripts

The production of IFN in response to viral infections is regulated by IFN regulatory factors (IRFs) such as IRF-3 and IRF-7 (Mamane *et al*., 1999). The IRFs are constitutively expressed and they translocate to the nucleus upon activation (Izaguirre *et al.*, 2003). Western blot analysis of the expression of IRF-3 and IRF-7 confirmed the constitutive expression of IRF-3 and IRF-7 in HEK 293H cells (Figure 6.5). Visual inspection suggests that IRF-3 seems to be slightly down regulated in SA11 mRNA-transfected HEK 293H cells (Figure 6.5).

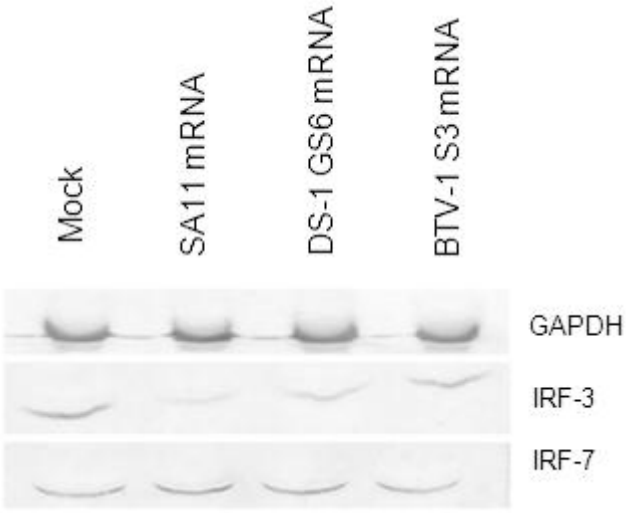

Figure 6.5. Western blot analysis of expression of interferon regulatory factors IRF-3 and IRF-7. The transcripts which were transfected i.e., a mock transfection, SA11 mRNA, DS-1 genome segment 6 (VP6) mRNA and BTV-1 S3 (VP3) mRNA are indicated at the top of each lane. A GAPDH control was included for each transfection (top strip) and IRF-3 expression is shown in the middle strip, while IRF-7 is shown in the bottom strip.

Interferons are a large family of multifunctional cytokines involved in antiviral defence (Randall and Goodbourn, 2008, Goodbourn *et al*., 2000). Viral infections induce type I (IFN-α and IFN-β) and type III (IFN-λ) interferon responses (Ank *et al*., 2006a, Samuel, 2001). These cytokines are stimulated by different viral ligands. Type I IFN mediate apoptotic cell death (Tanaka *et al.*, 1998). Since the cellular innate immune response to rotavirus transcripts has not been reported, this study determined the expression of IFN-α, IFN-β and IFN-λ1 in HEK 293H cells following the transfection of rotavirus transcripts and BTV-1 transcripts. The determination was achieved by measuring the relative quantities of each cytokine mRNA with qRT-PCR. To further

characterise the cell death observed in chapter 5, detection of the poly(ADP-ribose) polymerase 1 (PARP-1) which is involved in DNA repair was performed with western blot. However, immunoblot analysis indicated that PARP-1 was expressed in mock transfected cells as well as cells in which rotavirus DS-1 genome segment 6, SA11 or BTV-1 transcripts were transfected (result not shown).

Synthetic, T7 polymerase-derived rotavirus DS-1 genome segment 6 (GS6; VP6) mRNA and wild-type SA11 DLP-derived rotavirus transcripts induced high expression levels of IFN-λ1- and IFN-1β-encoding mRNA (Figure 6.6A and B). The relative gene expression of IFN-1β-encoding mRNA induced by synthetic rotavirus DS-1 GS6 transcripts was 13 000-fold, while that induced by rotavirus SA11 mRNA was 10 000-fold (Figure 6.6B). The induced expression levels of mRNA encoding for IFN-λ1 were higher than the expression levels of mRNA encoding IFN-1β i.e., 30 000-fold induction by synthetic rotavirus DS-1 GS6 mRNA, and 23 000-fold induction by wild-type SA11 mRNA (Figure 6.6A). The synthetic BTV-1 S3 mRNA also induced high expression of mRNA encoding for both IFN-λ1 and IFN-1β, at relative quantities of ~28000-fold and ~40000-fold respectively (Figure 6.6A and B). The relative quantities of mRNA encoding for IFN-λ1 and IFN-1β which were induced by BTV-1 S3 mRNA were higher than that induced by both the rotavirus DS-1 GS6 mRNA and rotavirus SA11 mRNA (Figure 6.6A and B).

The expression of *CXCL10* mRNA in HEK 293H cells was also induced by the rotavirus DS-1 GS6, SA11 and BTV-1 S3 transcripts. The relative mRNA quantities of *CXCL10* induced by DS-1 GS6, SA11 mRNA and BTV-1 S3 mRNA were 3 200-fold, 3 500-fold and 5 600-fold respectively (Figure 6.6C). The relative expression levels of *TNF-α* mRNA, were low compared to the mRNA encoding for IFN-1β, IFN-λ1, and CXCL10. The TNF-α-encoding mRNA levels were between 50-fold (DS-1 GS6 mRNA) and 100-fold (SA11 mRNA; Figure 6.6D). The highest relative quantity of *IFN-α* mRNA observed was 12-fold (induced by BTV-1 S3), while relative quantities induced by DS-1 GS6 mRNA and rotavirus SA11 were only 6- and 4-fold respectively (Figure 6.6G). The mRNA encoding the cytokines IL-10 (anti-inflammatory Th2-type), IL12 p40 and RIP1 expression levels were not significantly stimulated by rotavirus or BTV-1 S3 transcripts (Figure 6.6E, F and H).

A. *IFN-λ1* mRNA

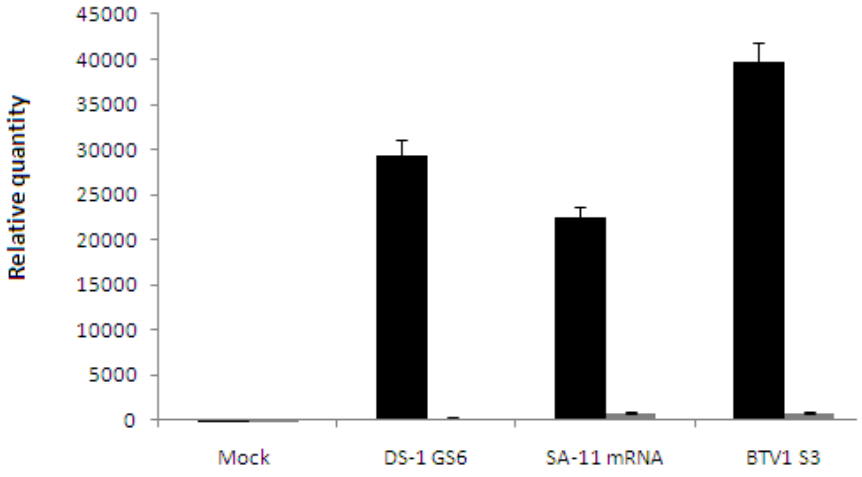

B. *IFN-1β* mRNA

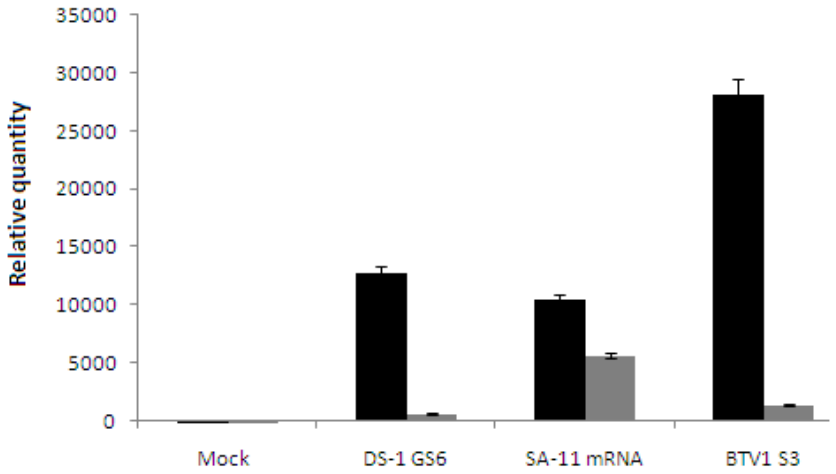

C. *CXCL10* mRNA

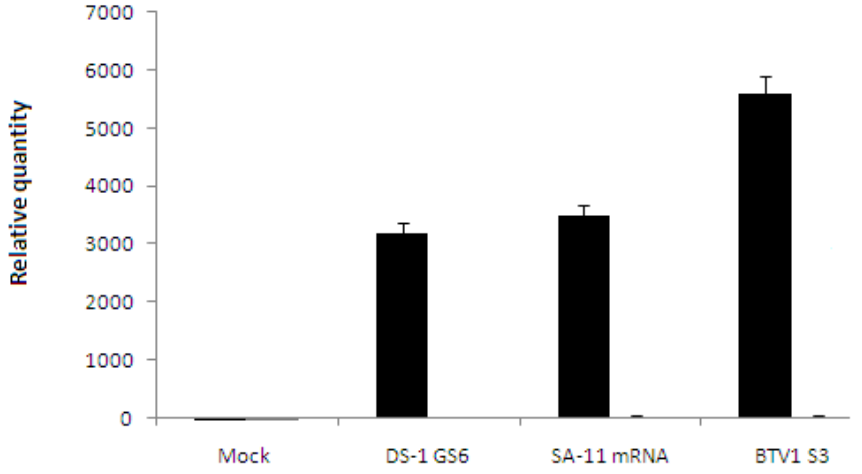

D. *TNF-α* mRNA

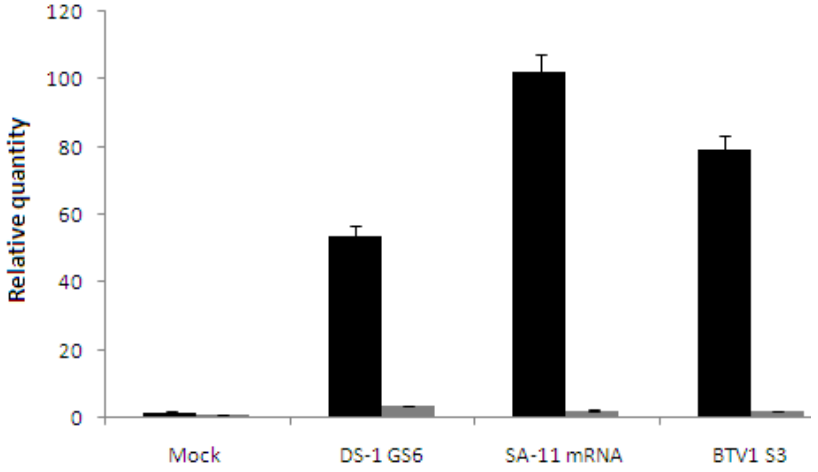

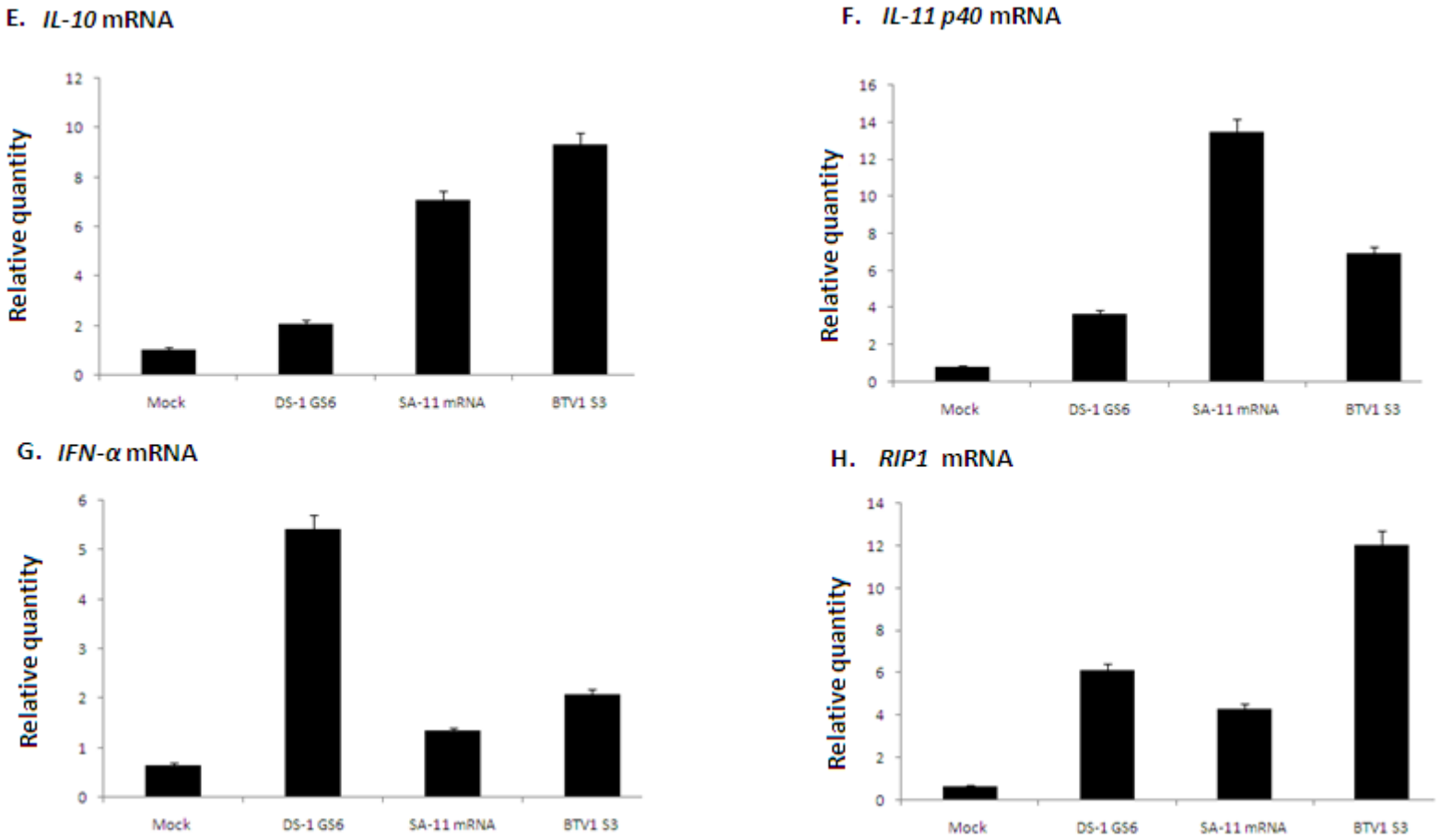

Figure 6.6. Relative quantities of cytokine-encoding mRNA expression induced in HEK 293H cells by rotavirus DS-1 genome segment 6, rotavirus SA11 and BTV1 S3 transcripts. The gray bars in graphs **A–D** indicate the effect of imidazolo-oxindole PKR inhibitor C16 on the induction of IFN-1β, IFN-λ1, CXCL10 and TNF-α, in HEK 293H cells by rotavirus DS-1, rotavirus SA11 and BTV1 transcripts. Graphs **E–H** show the relative quantities of mRNA encoding for IL-10, IL-11 p40, IFN-α and RIP1. Values were the arithmetic mean of three independent experiments and bars indicate the standard error of the mean.

The inhibition of the dsRNA-dependent kinase (PKR) improves the efficiency of recovery of BTV by reverse genetics (Attoui *et al*., 2009). The effect of inhibiting of the PKR system with imidazolo-oxindole PKR inhibitor C16, on the strongly induced cytokine mRNAs (encoding IFN-1β, IFN-λ1, CXCL10 and TNF-α), was investigated by transfecting rotavirus or BTV-1 transcripts in combination with inhibition of the PKR system with imidazolo-oxindole C16 PKR inhibitor (Jammi *et al*., 2003). PKR inhibition significantly reduced the levels of expression of *IFN-1β*, *IFN-λ*, *CXCL10* and *TNF-α* mRNA. *IFN-1β* mRNA levels were reduced from relative quantities of approximately 13 000-fold (DS-1 GS6), 10 000-fold (SA11 mRNA) and 28 000-fold (BTV-1) to ~700-, 6000- and 1400-fold respectively (Figure 6.6B). For IFN-λ1, the relative gene expression was reduced from ~30 000-fold (DS-1 GS6 mRNA), 23 000-fold (SA11 transcripts) and 40 000-fold (BTV-1 S3 transcripts) to ~300-fold for DS-1 GS6 mRNA, 800-fold for both SA11 and BTV-1 S3 mRNA (Figures 6.6A). The *CXCL10* mRNA expression levels were suppressed from relative quantities ranging between 3000- and 6000-fold to low levels between 14-fold and 42-fold (Figure 6.6C). The imidazolo-oxindole PKR inhibitor C16 further reduced the low induction of *TNF-α* mRNA (54–102-fold) to relative gene expression levels below 4-fold (Figure 6.6D). However, PKR inhibition did not completely abrogate the stimulation of IFN-1β, IFN-λ1and CXCL10 (Figure 6.6A–C). Furthermore, the attempt to determine the extent of PKR inhibition with western blot analysis was not conclusive due to the presence of smears (result not shown).

6.3 Discussion

Current literature describes the innate immune responses to rotavirus particles and dsRNA (Frias *et al*., 2010, Frias *et al*., 2012, Lopez and Arias, 2012, Angel *et al*., 2012, Deal *et al.*, 2010, Sen *et al*., 2011). In these studies, determinations of the innate immune responses were performed following the infection of animals or cells in culture (Sen *et al*., 2011, Sen *et al*., 2009, Gonzalez *et al*., 2010, Broquet *et al*., 2011, Pott *et al*., 2012, Deal *et al*., 2010). In some investigations, the immune response was also determined following the transfection of rotavirus dsRNA (Deal *et al*., 2010). However, the specific response to rotavirus transcripts has not been characterised. Furthermore, the observation of cell death which was indicated to be apoptosis by cell death analyses, suggested the involvement of the RIG-I pathway

and failure to recover viable rotavirus following the transfection of rotavirus transcripts (chapter 5) prompted investigation into the innate immune response elicited in response. A number of important innate immune responses were detected. These include identification of the sensor of rotavirus transcripts and the cytokine-encoding genes which are induced in response to rotavirus transcripts.

The detection of RIG-I, but not MDA5 by western blot analysis (Figure 6.4) suggested that rotavirus transcripts are sensed via the RIG-I pathway and not through MDA5. This result concurs with the observation in chapter 5 (section 5.2.4) that rotavirus transcripts were seemingly expressed more abundantly in the RIG-I deficient BSR cells when compared to COS-7 cells which express both RIG-I and MDA5. However, both RIG-I and MDA5 helicases share functional similarities in the induction of IFN production via the MAVS/IPS pathway (Yoneyama *et al*., 2005). Therefore, activation of RIG-I by rotavirus transcripts partly contributes to the high expression levels of IFN-1β and IFN-λ1 that were observed in this study. Other reports using the bovine rotavirus UK strain showed that both RIG-I and MDA5 are individually dispensable for IFN production in mouse embryonic fibroblasts (Sen *et al*., 2011). Despite being individually dispensable, a combined deficiency of RIG-I and MDA5 results in the attenuation of the early rotavirus-induced IFN responses (Sen *et al*., 2011). In this study, MDA5 could not be detected following the infection of HEK 293H cells with rotavirus DS-1 or SA11. Therefore, activation of MDA5 could either be associated with rotavirus strain differences or it is not activated by transcripts. For orthoreovirus (reovirus), both RIG-I and MDA5 are triggered (Loo *et al.*, 2008). However, the transfection of reovirus dsRNA into MEFs showed that the IFN-β response was dependent on RIG-I, but not MDA5 (Kato *et al*., 2008). A recent report demonstrated that infection of epithelial cells with bluetongue virus infection is specifically sensed and controlled by RIG-I and MDA5 leading to the induction of type I IFN (Chauveau *et al*., 2012). Another study showed that, in rotavirus-infected intestinal epithelial cells, RIG-I and MDA5 were important for signalling type I IFN (Broquet *et al.*, 2011). In the present study, the determination of RIG-I and MDA5 responses were based on transfecting transcripts, and not rotavirus particles. Studies using the ssRNA influenza virus showed that RIG-I preferred short viral RNA segments (Baum *et al*., 2010). The smallest segment in influenza virus is segment 8 which is 890 bp (Steinhauer and Skehel, 2002). Short dsRNA that are <300 bp act

as RIG-I ligands, while dsRNA which stimulate MDA5 are >2000 bp (Kato *et al*., 2008). Furthermore, dsRNA of ~1000 bp was found to activate IFN production in a RIG-I-dependent manner (Kato *et al*., 2008). Therefore, the detection of RIG-I and not MDA5 following the transfection of *in vitro*-derived rotavirus transcripts in the present study seems to suggests that the rotavirus transcripts fold into secondary dsRNA structures which only induce RIG-I.

The hypothesis that transfection of rotavirus transcripts induced an antiviral state was confirmed with observations that high expression levels of mRNA encoding for IFN-1β, IFN-λ1 and CXCL10 were stimulated following rotavirus transfection (Figure 6.6A, B and C). Since IFN-β induces apoptosis in various cell lines such as epithelial cells (Chawla-Sarkar *et al*., 2003, Chawla-Sarkar *et al*., 2001, Stawowczyk *et al*., 2011), the cell death observed (chapter 5) can most likely be attributed to IFN-induced apoptosis. Furthermore, the entry of rotavirus transcripts into the replication cycle (in addition to host cell protein synthesis) is likely to be compromised by the antiviral state and hence probably no rotavirus particles are formed despite the protein synthesis (chapter 5). Contrary to IFN-1β, the type I IFN-α was inefficiently induced by rotavirus transcripts (Figure 6.6.G). Strong induction of *IFN-α* in pDCs was shown to depend on the presence of rotavirus VP4, VP7 or both (Deal *et al*., 2010). The very low expression levels of *IFN-α* mRNA observed following transfection of rotavirus transcripts confirms the conclusion of Deal and co-workers, that the presence of rotavirus transcripts during virus replication impairs IFN-α production in pDCs (Deal *et al*., 2010). This conclusion followed the observation that TNF-α was produced in the presence of inactive particles, but not transcriptionally active particles (Deal *et al*., 2010).

Only a few studies have focused on the role of the recently discovered IFN-λ1 in rotavirus infections (Pott *et al*., 2012, Pott *et al*., 2011). This study demonstrates for the first time that rotavirus transcripts induce the expression of the *IFN-λ1* gene in cell culture. While IFN-1β and IFN-λ1 bind unrelated heterodimer receptors, both trigger similar responses through STAT-1 and STAT-2 (Sommereyns *et al*., 2008, Zhou *et al*., 2007b, Goodbourn *et al*., 2000). A wide range of interferon stimulated genes (ISGs) are subsequently activated. The ability to induce the antiviral state is shared by type I and type III IFN (Ank *et al*., 2006b). The IFNs are regulated by IFN

regulatory factors and the detection of IRF3 and IRF7 in both mock-transfected and transcripts transfected cells was consistent with previous reports and the well-established knowledge that these regulatory factors are constitutively expressed (Jiang *et al*., 2011, Sgarbanti *et al*., 2007, Izaguirre *et al*., 2003). The activation of the IRFs results in their phosphorylation and translocation into the nucleus (Randall and Goodbourn, 2008). A recent *in vivo* study in mice showed that rotavirus-induced IFN-λ determines the antiviral response in epithelial cells (Pott *et al*., 2011). It was observed that mice lacking IFN-λ receptors were highly susceptible to rotavirus infection with severe pathology (Pott *et al*., 2011). Furthermore, mice treated with IFN-λ1 expressed low levels of rotavirus antigens compared to high levels in mock-treated animals, suggesting that IFN-λ conferred a unique protective function (Pott *et al*., 2011). The high induction of the *IFN-λ1* mRNA observed from transfecting rotavirus transcripts (Figure 6.6A) correlates with the idea that IFN-λ is instrumental in the early defence of intestinal mucosa against rotaviruses (Sommereyns *et al*., 2008).

CXCL10 is IFN-inducible (Farber, 1997) and the observed high expression levels was expected following the observed high expression levels of *IFN-1β* and *IFN-λ1*. Significant quantities of CXCL10 were also observed in rotavirus infected pDCs (Deal *et al*., 2010). CXCL10 was found to impair replication of Coxsackie virus through the recruitment of natural killer cells (Yuan *et al*., 2009). In respiratory syncytial virus infections, CXCL10 augmented dendritic cell and $CD8^+$ T cell efficacy (Lindell *et al*., 2008). However, the significance of CXCL10 stimulation in cell culture in response to rotavirus transcripts is not known.

Low expression levels of *TNF-α* mRNA, encoding the pleiotropic (multi-functional) inflammatory cytokine, were detected (Figure 6.6D). In myeloid dendritic cells, the relative gene expression level observed after stimulation with bacteriophage Φ6 dsRNA of 58 bp–108 bp was considered efficient at <100-fold (Jiang *et al*., 2011). Long dsRNA in the range 308 bp–1080 bp were found to be inefficient at stimulating TNF-α (Jiang *et al*., 2011). This further supports the conclusion that the hairpin and stem loops formed in rotavirus transcripts are <300 bp. TNF-α initiates a caspase-independent necrotic cell death (Morgan *et al*., 2008). Observations that rotavirus down-regulates pro-inflammatory cytokines in calves (Aich *et al*., 2007), suggests

that proinflammatory cytokines are also important in the innate immune response against rotaviruses. However, the low induction of RIP1 kinase suggests that the transcript-induced cell death does not occur via a programmed necrotic cell death pathway (Hitomi *et al*., 2008).

While imidazolo-oxindole PKR inhibitor C16 suppresses the expression levels of IFN, the relative quantities observed after PKR inhibition may potentially be effective against reverse genetics due to the potency of IFNs. The suppression of cytokine mRNA expression following inhibition of PKR is consistent with the finding that PKR regulates IFN-β secretion during rotavirus infection (Sen et al., 2011). The reduction in the stimulation of *IFN-1β*, *IFN-λ*, *CXCL10* and *TNF-α* mRNA by the inhibiting of PKR also supports the hypothesis that secondary dsRNA structures are formed in rotavirus transcripts. For PKR to be activated, it interacts with dsRNA that is at least 11 bp up to 85 bp in length (Bevilacqua and Cech, 1996, Lemaire *et al*., 2008). Knowledge about RNA folding in living cells is limited due to the complex cellular environment and lack of appropriate study methods (Zemora and Waldsich, 2010). Therefore, it was not possible to establish which stage of rotavirus replication is negatively affected by PKR inhibition. The suppression of the PKR in BSR and COS-7 cells did not inhibit cell death and also did not result in virus recovery (chapter 5). This suggests that the PKR system is but one of the barriers to recovery of rotavirus by reverse genetics. Modulation of the cellular innate immune system by inhibiting PKR was found to significantly improve efficiency of reverse genetics for orthoreovirus (Attoui *et al*., 2009). The PKR inhibitor, 2-aminopurine, particularly enhanced efficiency of recovery and shortened the time for the appearance of plaques (Attoui *et al*., 2009). However, inhibition of PKR was reported to be unfavourable for rotavirus replication (Frias *et al*., 2012). Furthermore, rotavirus infection activates PKR which subsequently results in the phosphorylation of eIF2-α (Rojas *et al*., 2010, Montero *et al*., 2008, Trujillo-Alonso *et al*., 2011). The phosphorylation of eIF2-α is part of the early phase of apoptosis and also leads to the inhibition of host-cell translation (Bevilacqua *et al*., 2010, Saelens *et al*., 2001). Rojas and co-workers attributed the activation of PKR in rotavirus infected-cells to genomic dsRNA which escaped from viroplasms (Rojas *et al*., 2010). However, the results described in this chapter strongly suggest that rotavirus transcripts fold into secondary dsRNA structures which subsequently activate PKR.

The induction of all the cytokines discussed above shows that transfection of rotavirus transcripts efficiently activates the innate immune system through PKR and RIG-I. The cytokine production will inevitably result in the development of an antiviral state in transfected cells. Therefore, a model innate immune response pathway which summarises these observations is proposed (Figure 6.7). Secondary dsRNA structures formed in rotavirus transcripts activate PKR and RIG-I but not MDA5. As described previously, PKR subsequently activates NF-κB and the phosphorylation of eIF2-α leading to IFN induction and the inhibition of host-cell translation, respectively. This path could be blocked by oxindolo-imidazole PKR inhibitor C16 (Figure 6.7). On the other hand, activation of RIG-I results in the activation of IPS which in turn stimulates IFN-1β and IFN-λ1 production through NF-κB and IRF3 (Sen *et al.*, 2011, Randall and Goodbourn, 2008). The IFNs will also activate the secretion of CXCL10. The result of the inhibition of translation, IFN production and CXCL10 is an antiviral state (Figure 6.7).

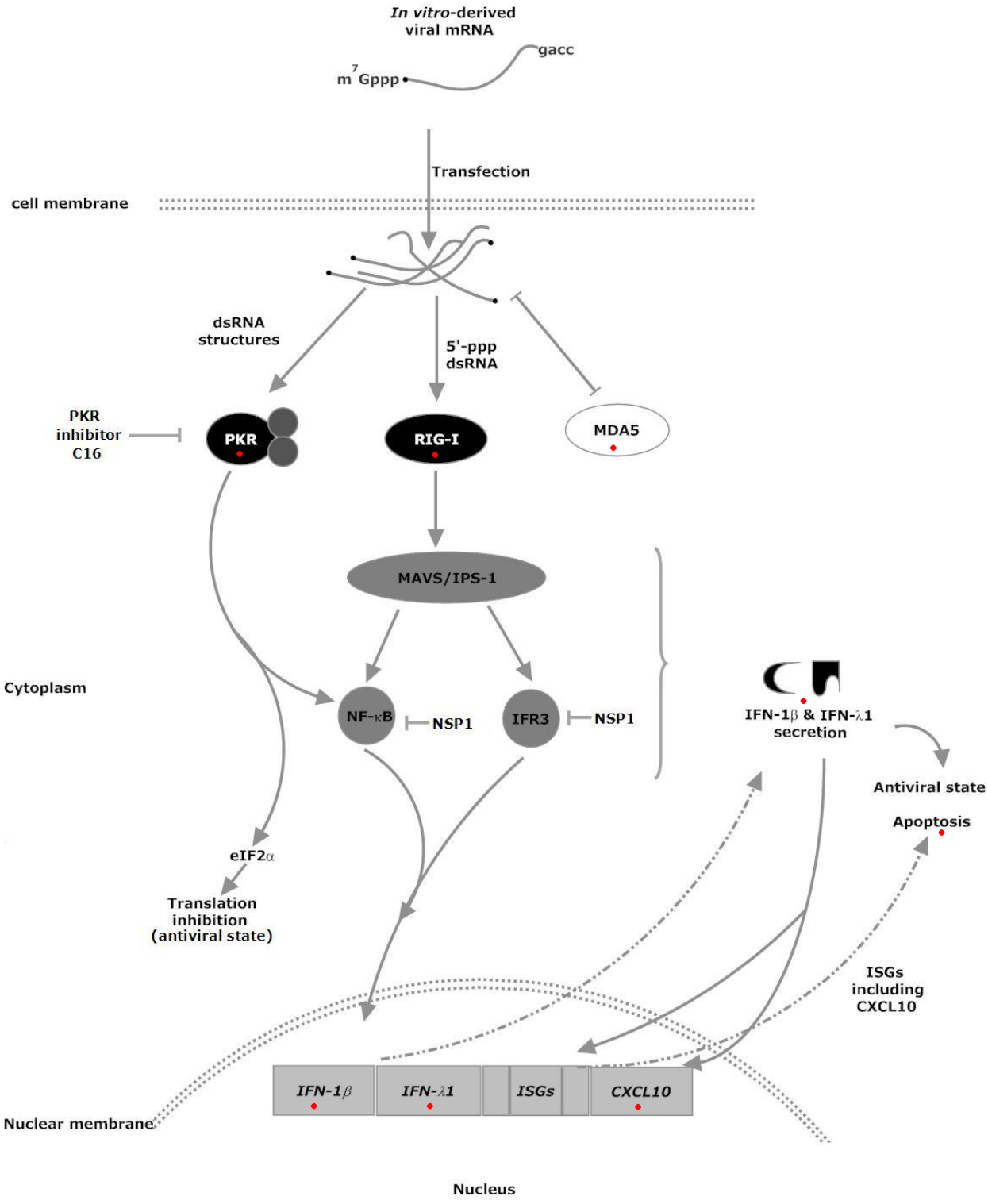

Figure 6.7. A proposed pathway depicting the interactions between transfected rotavirus DS-1 or SA11 transcripts and the innate immune system. The dotted arrows indicate nuclear gene responses. The interferon induced genes (ISGs) box is divided to indicate several ISGs which may be activated in response to interferon (IFN). The aspects of the pathway highlighted with red dots were investigated in this study. The part indicated by the bracket and establishment of the antiviral state are based on reports in the literature (Barro and Patton, 2005, Barro and Patton, 2007, Sen *et al*., 2011, Levy *et al.*, 2011).

In summary, HEK 293H were transfected with synthetic rotavirus DS-1 and wild-type rotavirus SA11 transcripts. Western blot analysis showed that the transcripts were sensed by RIG-I, but not MDA5. Strain variation and the presence of virus particles in infections may account for the involvement of MDA5 in other reports using whole-virus particles. Therefore, it is important to inhibit RIG-I or use cell lines that are RIG-I deficient in attempt to recover rotavirus by reverse genetics. Rotavirus mRNA derived from T7 polymerase and DLP *in vitro* transcription efficiently induced the expression of *IFN-1β* and *IFN-λ1* mRNA. This is the first demonstration that rotaviruses induce the *IFN-λ1* gene in cell culture. *CXCL10* mRNA is also strongly induced, as a consequence of IFN induction, but its role in cell culture is not known. These strongly stimulated cytokines are thought to contribute to an antiviral state in transfected cells and may partly contribute to rotaviruses being non amenable to a transcript-based reverse genetics system. The inhibition of PKR reduces the level of expression of mRNA encoding IFN-β, IFN-λ1, CXCL10 and TNF-α. However, PKR inhibition did not completely abrogate expression of *IFN-1β* and *IFN-λ1* mRNA. Since inhibiting PKR was found to reduce rotavirus replication efficiency, it may not be the best approach for use in a transcript-based rotavirus reverse genetics system. The transfection of rotavirus transcripts into cells in which the cytokines IFN-β, IFN-λ1, CXCL10 and TNF-α are deficient or inhibited needs further investigation. This could help in the strategic development of a transcript-based reverse genetics system for rotaviruses.